Possible evidence for exchange effects in the $^{16}O(^6Li, \alpha)^{18}F$ reaction at $E_{^6Li} = 34$ MeV†

G. E. Moore* and K. W. Kemper
Physics Department, The Florida State University, Tallahassee, Florida 32306
(Received 1 March 1976)

Fifty-four-point angular distributions in the angular range 2.5° to 170° have been measured for the $^{16}O(^6Li,\alpha)^{18}F$ reaction to the 1^+ (0.0 MeV), 3^+ (0.937 MeV), and $0^- + 5^+$ (1.1 MeV) states in ^{18}F at a bombarding energy of 34 MeV. In addition, forward angle data have been measured for the 2^- (2.101 MeV), 1^+ (3.725 MeV), 3^- (3.791 MeV), and 2^+ (3.836 MeV) states. The angular distributions for all of the above states are forward peaked and have little structure at back angles. The general structure of the first 60° of the angular distributions can be reproduced by zero-range two-particle transfer distorted-wave Born-approximation calculations; however, the calculations are generally 3° and as much as 10° out of phase with the data past the first maximum. A zero-range distorted-wave Born-approximation normalization factor of 100 is obtained assuming the 5^+ state to be a pure $(d_{5/2})^2$ configuration. Finite-range distorted-wave Born-approximation calculations which include the $2S$ and $1D$ components of ^6Li do not improve the fits to the data and are similar to zero-range calculations at forward angles. The $1D$ component was shown to have little effect on the calculated angular distributions. The absolute magnitudes of the cross sections are predicted to within a factor of 2 when the ^{18}F shell model wave functions of Kuo and Brown are used in the finite-range distorted-wave Born-approximation calculations. Two-particle and cluster form factors used in the finite-range calculations gave equivalent fits to the data. The magnitude of the cross section at angles greater than 90° and the phase of the forward angle data could not be reproduced by any of the calculations. The failure of the distorted-wave Born-approximation calculations at back angles suggests that a more complete description of the reaction mechanism which includes the exchange of an α particle in ^{16}O with the ^6Li projectile is necessary.

[NUCLEAR REACTIONS $^{16}O(^6Li, \alpha)^{18}F$, $E = 34$ MeV; measured $\sigma(\theta)$ $\theta = 2.5°$–170° lab, $\Delta\theta = 2.5°$; compared data to zero-range and finite-range DWBA calculations using shell model wave functions. Extracted (^6Li, α) zero-range normalization factor.]

I. INTRODUCTION

Previous measurements by White *et al.*[1] concluded that the $^{12}C(^6Li, \alpha)^{14}N$ reaction is principally a direct reaction at 33 MeV. However, the distorted-wave Born-approximation (DWBA) analysis of the $^{12}C(^6Li, \alpha)^{14}N$ reaction[2] was unsuccessful in reproducing the experimental angular distributions. The difficulties were attributed to the possibility of multistep contributions arising from the strong coupling between the ground and first excited states of the deformed nucleus ^{12}C.

In the present work, detailed measurements of the $^{16}O(^6Li, \alpha)^{18}F$ reaction at a bombarding energy of 34 MeV are reported. The ^{16}O target nucleus was chosen for this present study because of its very nearly spherical shape. Complete angular distributions for $^{16}O(^6Li, \alpha)^{18}F$ were obtained for the 1^+ (0.0 MeV), 3^+(0.937 MeV), and 5^+ (1.122 MeV) states in ^{18}F. These states were chosen because they have comparatively simple structures.[3] Excitation functions from 33 to 34.5 MeV bombarding energy were also taken. Both zero-range and finite-range distorted-wave Born-approximation (DWBA) calculations were performed for the states studied. A comparison is made with other detailed ($^6Li, \alpha$) data[2] and also with light ion ($p+n$) transfer reactions[4,5] to ^{18}F.

II. EXPERIMENTAL PROCEDURE

An inverted sputter source[6] was used to obtain a negatively charged lithium beam for injection into the Florida State University super FN tandem Van de Graaff accelerator. Average beam currents of 600 nA of $^6Li^{+++}$ were obtained on target. The targets used in this work were 50 $\mu g/cm^2$ Al_2O_3 films made by electron gun bombardment of a sapphire crystal. These targets did not result in appreciable energy straggling of the ^6Li projectiles and they easily withstood an 800 nA ^6Li beam for as long as 25 hours.

The large positive Q value (+6.054 MeV) of the $^{16}O(^6Li, \alpha)^{18}F$ reaction makes it possible to use a single Si surface barrier detector when measuring the α particles populating the low-lying states of ^{18}F since the α particles have the highest energy of all the reaction products over most of the angular range. Data were taken at laboratory angles of 2.5°, 3°, 80°, and 100° and in the angular ranges 5° to 72.5° and 110° to 170° in 2.5° increments. A quadrupole spectrometer[7] was used to take data forward of 15°, while data at other angles were ob-

tained in a large volume scattering chamber.[8]

An array of six Si surface barrier detectors was used simultaneously to take data in the scattering chamber. The thicknesses of the detectors were 1500, 700, 380, and 300 μm and were chosen so that the highest energy tritons, deuterons, and protons would not be stopped in the counters. The detectors, mounted 10° apart in an aluminum wedge, were cooled to −20°C. The ^{16}O elastic scattering yield from a stationary monitor counter was used to correct the data for fluctuations in target thickness and current integration. The detector collimation was such that a solid angle of 0.19 msr and an angle of 0.26° were subtended. The small polar angle was necessary to reduce the large kinematic broadening of the detected α particles. Spectra were also taken with $\Delta E \times E$ Si surface barrier counter telescopes to make certain that in the region of interest the single counter spectra did not have any contaminant peaks from other particle types.

The quadrupole spectrometer was used to obtain higher resolution spectra [~45 keV full width at half maximum (FWHM)] at forward angles. An angle of 0.56° and solid angle of 0.51 msr were subtended for charged particles by the single 1500 μm silicon surface barrier detector placed at the focal position of the spectrometer. The collimation was such that a uniform efficiency was obtained for particles within half an MeV of the focused energy. The quadrupole spectrometer was set to focus the 5^+ (1.119 MeV) state of ^{18}F for the angular distribution measurements. Absolute cross sections were obtained by normalizing to data taken at 15°, 17.5°, and 20° in the scattering chamber.

The signals from the detectors were amplified with active filter and biased amplifiers and then pulse height analyzed by analog-to-digital converters interfaced via CAMAC to an EMR-6130 computer. The data were written on magnetic tape for off-line peak fitting using a Gaussian peak fitting program controlled by an interactive light pen.

The relative statistical and peak fitting errors in the cross sections are represented by the error bars on the individual data points for the angular distributions. The product of solid angle and target thickness for the ^{16}O(^{6}Li, α)^{18}F reaction data were determined by measuring the elastic scattering yield of 4.5 MeV protons scattered by ^{16}O at an angle of 30° c.m. where the cross section has been previously measured by Salisbury *et al.*[9] The excitation function for proton scattering is structureless between 4.4 and 4.6 MeV. The resulting error in the determination of the absolute cross section for the ^{16}O(^{6}Li, α)^{18}F reaction is 8%, which arises from the quadrature addition of the following errors: absolute cross sections from Ref. 9 (0.5%), extraction from the graphs of Ref. 9 (2.5%), current integration for each run (5%), statistical and background determination error in the proton yield (1.5%), and statistical and background determination error in the extraction of the ^{16}O(^{6}Li, α)^{18}F reaction yields (2.9%).

III. EXPERIMENTAL RESULTS

A. States populated

An α-particle spectrum obtained with a single counter at the focal position of the quadrupole spectrometer for states of ^{18}F is shown in Fig. 1 for the ^{16}O(^{6}Li, α)^{18}F reaction. This spectrum is the combined result of data taken at two focal settings. Higher-lying states of ^{18}F were observed with a counter telescope in the scattering chamber and a typical spectrum is shown in Fig. 2. The spins, parities, and excitation energies of known states in ^{18}F are given in Table I along with a comparison of the cross sections for the ^{16}O(^{6}Li, α)^{18}F, ^{16}O(^{3}He, p)^{18}F, and ^{16}O(α, d)^{18}F reactions. The (^{6}Li, α) reaction generally populates states with the same relative intensities as those populated in the (^{3}He, p) reaction but with about a 10th the magnitude observed in the (^{3}He, p) reaction.

Complete angular distributions were obtained for states (or groups of states) at 0.0, 0.937, and 1.1 MeV excitation energy, while partial angular distributions were obtained for groups of states at 2.101, 3.725, 3.791, and 3.836 MeV excitation energy in ^{18}F. The peak at 1.1 MeV is an unresolved doublet. The shape of this peak was observed to broaden and shift its centroid at forward angles as seen in Fig. 3 indicating the presence of the two known states, 0^- (1.081 MeV) and 5^+ (1.122 MeV). The characteristic $L = 1$ transfer of the 0^- state would account for its presence at extreme forward angles compared with the 5^+ state, producing the broadened peak.

No evidence for the population of the 0^+ (1.042 MeV), $T = 1$ state, which is forbidden both by isospin and spin selection rules, was observed. The 2^+ (3.060 MeV) state, which is forbidden by isospin selection rules, was also not observed.

The negative parity states at 2.101 and 3.791 MeV were observed to be weakly populated relative to the positive parity states. The 2^- (2.101 MeV) state, which has been assigned[5] a $p^{-1}(sd)^3$ configuration, was observed to be strongest at forward angles where it has about a fifth of the cross section of the 1^+ (0.0 MeV) state. The 3^- (3.791 MeV) state is in a triplet of states that was only resolved for spectra obtained with the single counter in the quadrupole. This state can arise from either a particle-hole configuration or a low-lying $1f_{7/2}$

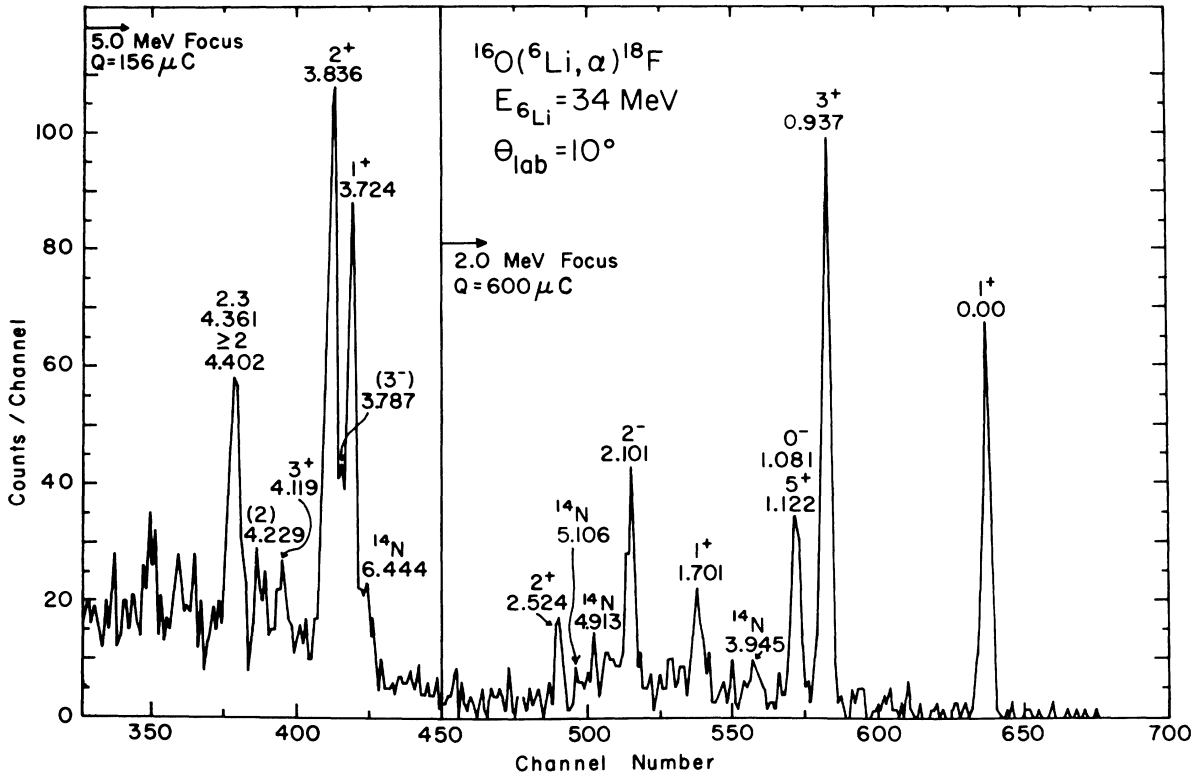

FIG. 1. A composite spectrum for the reaction $^{16}O(^6Li, \alpha)^{18}F$ obtained with the quadrupole spectrometer. The quadrupole was set to focus α particles populating excitations in ^{18}F of 2.0 and 5.0 MeV.

component in the ^{18}F wave function. At forward angles the cross section to the 1^+ (3.725 MeV) and 2^+ (3.836 MeV) states are nearly equal in magnitude and greater than that of the 3^- (3.791 MeV) state. The 1^+ (1.701 MeV), 2^+ (2.524 MeV), and 1^- (3.135 MeV) states were assigned[5] as having particle-hole configurations and they are all weakly populated in the $^{16}O(^6Li, \alpha)^{18}F$ reaction. Peaks were observed in the spectra at excitation energies of 4.119, 4.229, 4.4, 5.61, 6.11, 6.20, 6.53, 6.80, and 6.88 MeV as seen in Figs. 1 and 2; however, it was not possible to resolve individual higher-lying states because of the high density of states.

The experimental angular distribution for the $^{16}O(^6Li, \alpha)^{18}F$ reaction to the 1^+, ground state is compared with angular distributions to 1^+ states in the $^{12}C(^6Li, \alpha)^{14}N$ reaction[2] in Fig. 4. The angular distribution for the 0.0 MeV state in ^{14}N is out of phase with the other 1^+ angular distributions at forward angles as expected from $(^3He, p)$ studies.[4,5,11,12] The $(^3He, p)$ reaction studies have shown all of these 1^+ transitions to have predominately $L = 0$ shapes, except for the 0.0 MeV state in ^{14}N which is predominately $L = 2$. The 6.200 MeV state in ^{14}N and the 0.0 MeV state in ^{18}F have almost identical shell model configurations and their angular distributions are also similar as can be seen in Fig. 4.

Angular distributions for the 3^+ states are shown in Fig. 5. Angular distributions from $(^3He, p)$ reactions to these states have been shown to be predominately $L = 2$. The nuclear structure of both of these states is believed to be similar and the angular distributions for the two $(^6Li, \alpha)$ reactions are also similar.

B. Compound nucleus effects

Compound nuclear contributions have been shown to be small in the $^{12}C(^6Li, \alpha)$ reaction at bombarding energies above 30 MeV by White *et al.*[1] They observed "flat" yield curves in the energy range 32–36 MeV for the first nine $T = 0$ states in ^{14}N at angles of 15° and 65° for $^{12}C(^6Li, \alpha)^{14}N$. Fluctuations in the $^{16}O(^6Li, \alpha)^{18}F$ reaction cross section between 20 and 26 MeV have been observed[13] to be less than 20% for states of excitation energies 0.0, 0.927, 1.1, 1.701, and 3.8 MeV at angles of 15° and 65°. Yields were measured in the present work between 33.0 and 34.5 MeV in 0.1 MeV increments at angles of 20°, 30°, and 170°. The 20° and 170° data are shown in Fig. 6. The sum of the energy

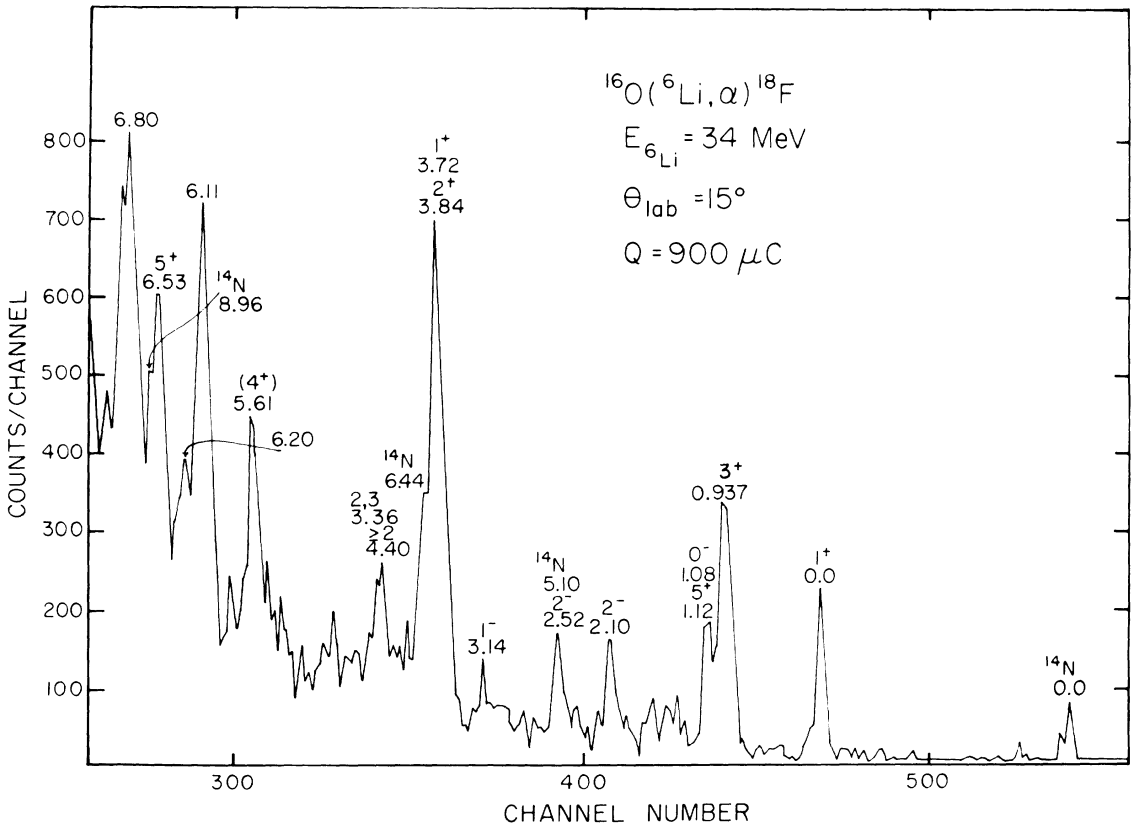

FIG. 2. Sample spectra from the $^{16}O(^{6}Li, \alpha)^{18}F$ reaction taken with a counter telescope in a scattering chamber. States up to 6.80 MeV in excitation energy were observed.

stability of the ^{6}Li beam and energy loss in the target was less than 35 keV for these data. The excitation functions are rather structureless. As seen in Fig. 7, which is a best resolution spectrum at 170°, the 1^+ (0.0 MeV), 3^+ (0.937 MeV), and 1.1 MeV states are decidedly more pronounced than any other states. The 1^+ (1.701 MeV) state which has a particle-hole configuration is never more than one-fifth as intense as the ground state over the entire angular and energy range studied. If the $(^{6}Li, \alpha)$ reaction were compound at back angles, the 1^+ (1.701 MeV) state would have the same intensity as the ground state. Consequently, the compound nucleus contribution in the ground state can be no more than 20% and is neglected in the analysis of the $(^{6}Li, \alpha)$ data for the strongly populated states.

IV. DWBA ANALYSIS

A. DWBA formalism

The differential cross section for a stripping reaction $A(a,b)B$, in which $a = b + c$ and $B = A + c$ is expressed[14] using the distorted-wave Born approximation as

$$\frac{d\sigma}{d\Omega} = \frac{\mu_a \mu_b}{(2\pi\hbar^2)^2} \frac{k_b}{k_a} \frac{(2I_B+1)(2I_b+1)}{(2I_A+1)(2I_a+1)} \sum_{L I_p I_t} \sigma_{L I_p I_t}(\theta) , \tag{1}$$

where

$$\sigma_{L I_p I_t}(\theta) = \sum_M |\beta^{LM}_{I_p I_t}|^2 . \tag{2}$$

The total angular momentum of nuclei A, B, a, and b are given by I_A, I_B, I_a, and I_B, respectively. The quantum numbers L, M, I_p, and I_t refer, respectively, to the angular momemtum transfer, projection of the angular momentum transfer, total angular momentum transferred to the target A by c in forming the residual nucleus B, and the total angular momentum stripped from the projectile a in the formation of the emitted particle b. The reduced mass and wave number of incident and exit channels are given by μ and k for the respective channels. The stripping amplitude $\beta^{LM}_{I_p I_t}$ is expressed in the post formalism as

TABLE I. A comparison of states populated in the (^{6}Li,α), (^{3}He,p), and (α,d) reactions. Curly brackets indicate clusters of unresolved states. The cross section is placed where the strongest state is expected.

E_x [a]	J^π [a]	T [a]	$\frac{d\sigma}{d\Omega}$(^{6}Li,α) [b] (mb/sr)	σ_T(^{3}He,p) [c] (mb/sr)	σ_T(α,d) [c] (mb/sr)	Dominant [c] configuration	Dominant [c] L
0.0	1^+	0	0.24	2.42	0.85	$(s,d)^2$	0
0.937	3^+	0	0.43	6.10	1.89	$(s,d)^2$	2
1.042	0^+	1	...	...	...	$(s,d)^2$	0
1.081	0^-	0	{ ...	} ...	{ ...	$(p)^{-1}(s,d)^3$	...
1.122	5^+	0	0.15	4.96	8.46	$(s,d)^2$	4
1.701	1^+	0	<0.07	0.45	0.13	$(p)^{-2}(s,d)^4$	0
2.101	2^-	0	0.12	1.05	0.27	$(p)^{-1}(s,d)^3$	...
2.524	2^+	0	0.15	0.46	0.10	$(p)^{-2}(s,d)^4$	2
3.060	2^+	1	...	{ 3.04	...	$(s,d)^2$	2
3.135	1^-	0	<0.01	{ ...	0.13	$(p)^{-1}(s,d)^3$	...
3.357	3^+	0	...	0.70	0.22	$(s,d)^2$	...
3.725	1^+	0	0.27	...	...	$(s,d)^2$	...
3.791	(3^-)	0	0.1	} ...	{ ...	$(p)^{-1}(s,d)^3$	...
3.836	2^+	0	0.63	6.41	0.89	$(s,d)^2$	2
4.119	3^+	0	...	{ 1.02	{ 0.44	...	...
4.229	(2)	...	...	{ ...	{ ...	...	...
4.361	2,3	...	...	{ ...	{ ...	...	...
4.402	≥ 2	0	...	{ 1.90	{ 0.55	...	...
4.650	4^+	1	...	{ 2.45	...	$(s,d)^2$	4
4.739	0^+	1	...	{ ...	...	$(s,d)^2$	...
4.849	1	0	...	1.36	0.55	...	...
4.957	2^+	1	...	0.61	...	$(s,d)^2$	...
5.301	4^+	0	...	0.48	{ ...	...	...
5.501	...	...	...	...	{ ...	...	...
5.599	(4^+)	0	{ 0.24	{ 2.71	{ 0.37	$(s,d)^2$	...
5.606	1^-	0,1	...	{ ...	{ ...	...	...
5.674	1^-	0,1	...	...	{ ...	...	...
5.785	$T=0$		...	...	{ ...	...	...
6.095	4^-	0	0.63	5.62	{ ...	...	...
6.135	0^+	1	...	...	{ 1.68	...	...
6.161	3^+	1	...	...	...	...	...
6.240	(3^-)	...	{ 0.1	...	...	...	...
6.261	(1)	...	} ...	{ 3.38	...	...	...
6.280	2^+	...	...	{ ...	...	...	...
6.309	$2^+,3^+$	...	...	...	...	...	...
6.385	$(1^+),2,3^-$	...	...	...	...	...	...
6.483	$(1^+),2,3^-$	...	...	...	...	...	...
6.565	5^+	0	0.3	...	0.60	...	...
6.646	1^-	...	...	...	...	...	...
6.647	(2^-)	...	...	...	...	...	...
6.780	$4^+,5^+$	0	...	...	{ ...	...	...
6.808	$2^+,3^+$	...	{ ...	{ ...	{ 1.17	...	...
	2^-	0	{ 0.8	{ 7.67	...	...	...

[a] See Ref. 10.

[b] Cross section at $\theta_{lab}=15°$ in the present work.

[c] See Ref. 5. Cross sections taken at ^{3}He = 19.8 MeV and E_α = 40.3 MeV, are integrated from $\theta_{c.m.}=12°-80°$.

$$\beta^{LM}_{I_pI_t}=\frac{i^{-L}}{(2L+1)^{1/2}}\int \chi^{(-)}_{bB}{}^*(\vec{k}_b,\vec{r}_{Bb})F^{LM}_{I_pI_t}(\vec{r}_{Ac},\vec{r}_{bc}) \times \chi^{(+)}_{aA}(\vec{k}_a,\vec{r}_{Aa})d^3r_{Ac}d^3r_{bc}\ , \quad (3)$$

where $\chi^{(-)}_{bB}$ and $\chi^{(+)}_{aA}$ are the distorted waves for exit and incident channels. The form factor $F_{LI_pI_tM}$ contains the wave functions of the particle c bound to both b and A. In the present case, c represents two nucleons. To facilitate computation of the integral in Eq. (3), the two-particle wave functions are transformed into relative and center of mass coordinates by using the Moshinsky transformation.

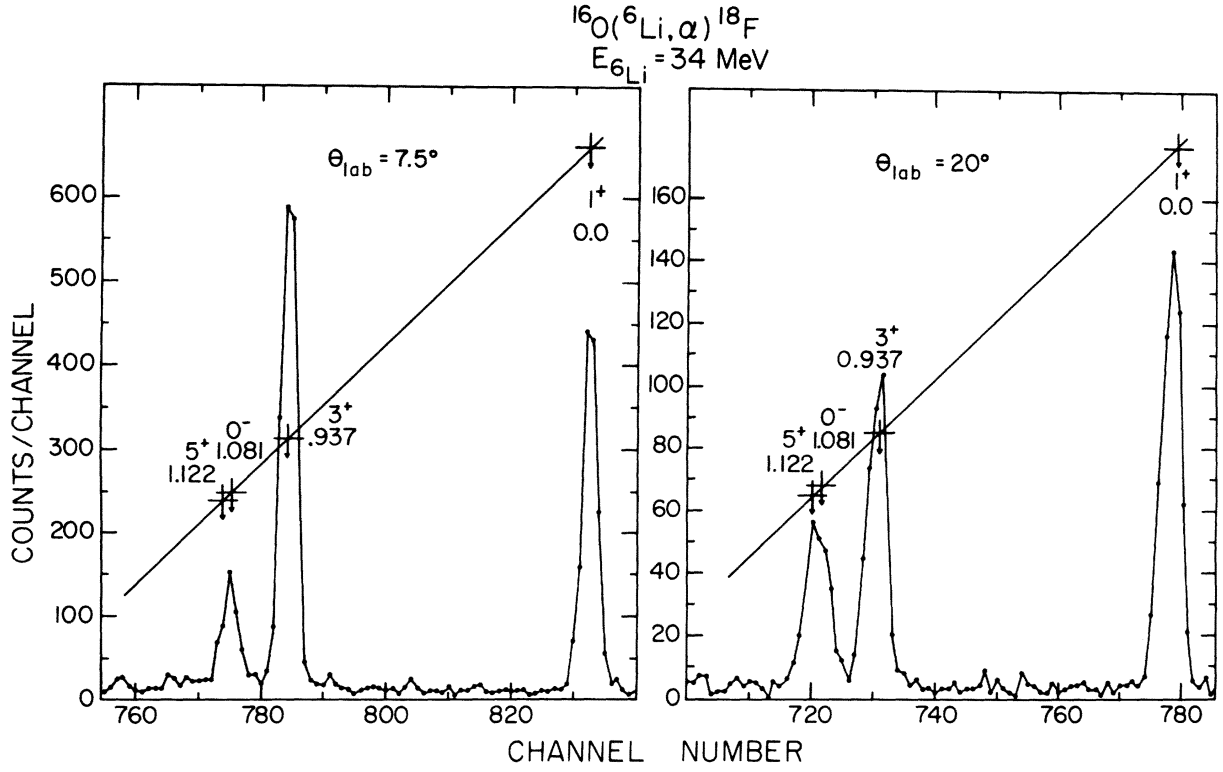

FIG. 3. A comparison of α-particle spectra for the 0.0, 0.937, 1.081, and 1.122 MeV states in ^{18}F at 7.5° and 20° lab angle obtained with the quadrupole spectrometer. The centroid of the doublet at 1.1 MeV shifts to the position of the 1.081 MeV state at forward angles.

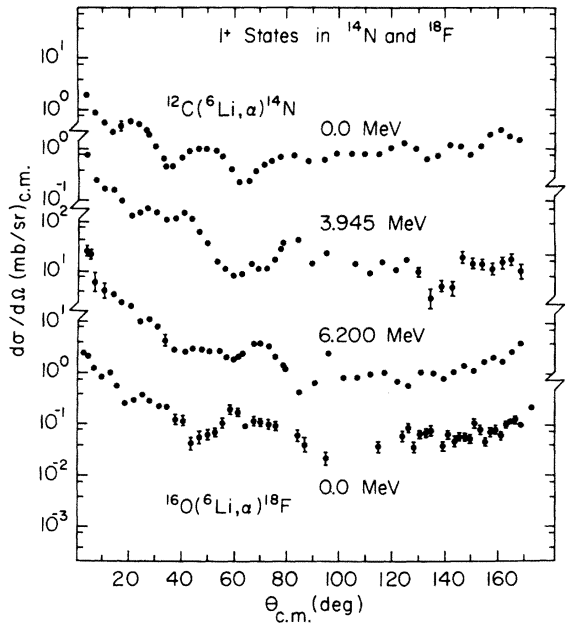

FIG. 4. A comparison of angular distributions for the $^{16}O(^6Li, \alpha)^{18}F$ and $^{12}C(^6Li, \alpha)^{14}N$ reactions.

The two particles then have relative motion quantum numbers with respect to the cores A and b given by N_tL_t and N_bL_b, respectively. These cluster quantum numbers are related to the shell model node and angular momentum quantum numbers n

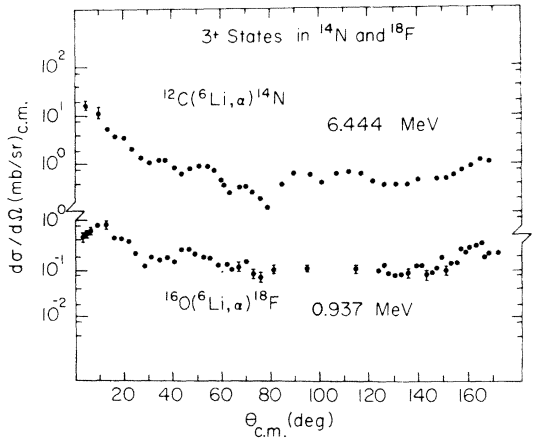

FIG. 5. A comparison of angular distributions of 3^+ states for the $^{16}O(^6Li, \alpha)^{18}F$ and $^{12}C(^6Li, \alpha)^{14}N$ reactions.

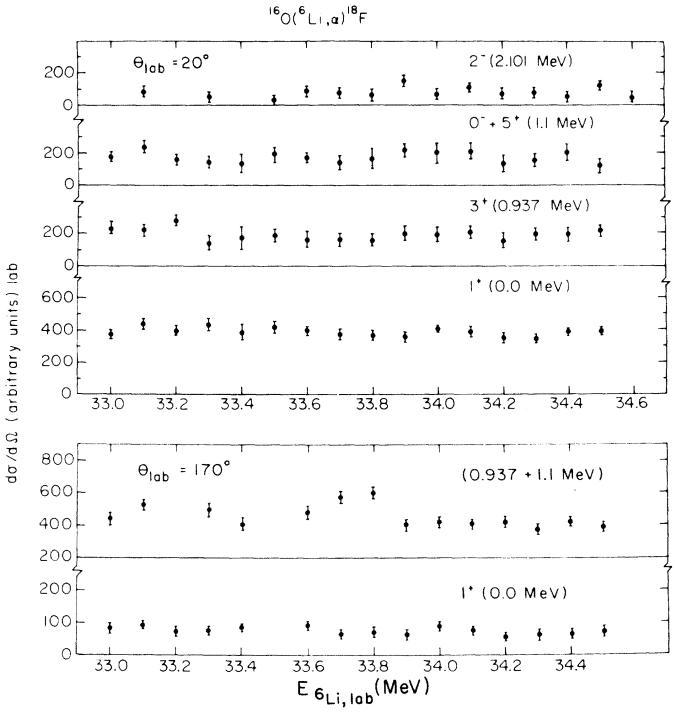

FIG. 6. Yield curves for the 1^+ (0.0 MeV), 3^+ (0.937 MeV), $0^- + 5^+$ (1.1 MeV) and 2^- (2.101 MeV) states in ^{18}F at the lab angles 20° and 170°.

and λ of occupied states by

$$2N_t + L_t = \sum_{i=1}^{2} (2n_i + \lambda_i) \tag{4}$$

for the target and

$$2N_p + L_p = \sum_{j=1}^{2} (2n_j + \lambda_j) \tag{5}$$

for the projectile. Additionally, the vector sum of L_t and L_p form the angular momentum transfer L. The sum over L, I_p, and I_t in Eq. (1) is incoherent. The sum over L_p and L_t that form a single value for L is coherent. The cluster wave function of $^6Li(\alpha + d)$ taken from a previous analysis of ^6Li-$(p, ^3He)^4He$ experimental data[15] gives a $2S$ component with amplitude 0.8 and a $1D$ component with amplitude 0.2.

The form factor in Eq. (3) expressed in terms of the nuclear structure factor $G(N_tL_tSI_tT_t)$, interaction potential $V(r_{bc})$ radial wave function of c bound to A, $\Phi_{N_tL_t}(\vec{r}_{Ac})$, radial wave function of c bound to b, $\Phi_{N_pL_p}$, and amplitude $\alpha_{N_pL_p}$ is given by

$$F_{LI_pI_tM}(\vec{r}_{Ac}\vec{r}_{bc}) = \sum_{\substack{N_pL_p \\ N_tL_t}} \frac{i^L(-1)^{L_t+I_t-I_p+M}(2L+1)^{1/2}(2I_a+1)^{1/2}}{(2I_b+1)^{1/2}} W(L_tLI_cI_p;L_pI_t)G(N_tL_tSI_tT_t)\alpha_{N_pL_p}V(r_{bc})$$
$$\times [(-1)^M \Phi^*_{N_tL_t}(\vec{r}_{Ac})\Phi_{N_pL_p}(\vec{r}_{bc})]^L_M \,. \tag{6}$$

If α_{1D} for ^6Li is much less than α_{2S} and the spatial extent of ^6Li can be reduced to a δ function, then the zero-range approximation can be used to determine the scattering amplitude.

B. DWBA calculations

1. Optical model parameters

Schumacher *et al.*[16] have obtained two sets of optical parameters from fits to elastic scattering of

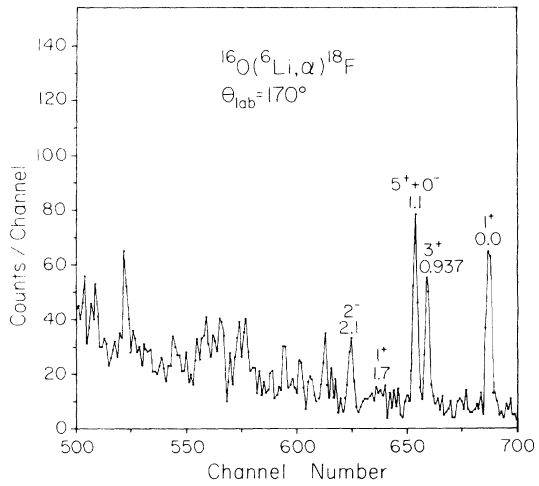

FIG. 7. A best resolution spectrum for the $^{16}O(^6Li, \alpha)$-^{18}F reaction taken at an angle of 170° lab.

^6Li by ^{16}O at $E_{^6Li} = 34$ MeV. There parameters, given as Sets I and II in Table II were used in Ref. 16 in a DWBA analysis of the $^{16}O(^6Li, ^7Li)^{15}O$ reaction. Somewhat better fits were obtained with Set I rather than Set II for this case. Both sets are investigated in the $^{16}O(^6Li, \alpha)^{18}F$ reaction analysis presented here.

The α-particle elastic scattering parameters are more ambiguous because ^{18}F is not stable, so the needed elastic scattering measurement cannot be carried out. Harvey, Meriwither, and Mahoney[17] have used the optical model to fit 40.5 MeV α-particle elastic scattering by ^{18}O in the angular range 10° to 60° c.m. Hansen *et al.*[18] have obtained optical model parameters from fits to 28.5 MeV α particles elastically scattered by ^{20}Ne. The parameters of Hansen *et al.* have been used by Obst and Kemper[19] in coupled-channels Born-approximation calculations for the $^{19}F(\alpha, t)^{20}Ne$ reaction at 28.5 MeV. The two optical model parameter sets of Harvey *et al.*[17] and Hansen *et al.*[18] are also given in Table II as α-particle sets I and II, respectively.

2. *Shell model wave functions of* ^{18}F

The wave functions of Kuo and Brown[3] for the low-lying positive parity states of ^{18}F are given in Table III. The structure factors $G(N_t L_t, S=1, I_t T_t = 0)$ have been calculated by Mangelson[5] from these wave functions and are given in Table IV. These structure factors have been used by Polsky *et al.*[4] in cluster model DWBA calculations for the $^{16}O(^3He, p)^{18}F$ reaction. The 5^+ (1.122 MeV) state has a pure $(1d_{5/2})^2$ or $L_t = 4$ configuration, which makes it an interesting state to study. Also, the 1^+ (0.0 MeV), 3^+ (0.937 MeV), and 2^+ (3.836 MeV) states have one dominant L value in the cluster representation.

3. *Zero-range* DWBA *calculations*

The initial analysis of the data was made in terms of the zero-range DWBA. These calculations, denoted by ZRTNT, were performed using the two-nucleon form factor option of the computer program DWUCK.[20] This option performs the transformation to relative and center of mass coordinates according to the method of Bayman and Kallio.[21] The ^{18}F wave functions of Table II are used in conjunction with single-nucleon radial wave functions generated from a Woods-Saxon potential. The radial integrations were carried out to 20 fm in 0.1 fm steps and 30 partial waves were included in the calculations presented in this work.

Zero-range DWBA calculations for the 1^+ (0.0 MeV) state of ^{18}F were used initially to examine the sensitivity of the $^{16}O(^6Li, \alpha)^{18}F$ results to the optical and bound state potentials. The magnitude and phase of the calculated angular distributions was found to be similar with either set of ^6Li optical parameters in conjunction with each of the α-particle optical parameter sets. Sets I and IV produced angular distributions with somewhat deeper minima at back angles.

Further DWBA calculations for the 3^+ (0.937 MeV) and 5^+ (1.119 MeV) states reflected the same insensitivity to choice of optical parameters. The

TABLE II. Optical model parameters.

Particle	Set	U (MeV)	r_r [a] (fm)	a_r (fm)	W (MeV)	r_i [a] (fm)	a_i (fm)	r_c (fm)	Ref.
^6Li	I	164.3	1.21	0.826	10.6	2.017	1.086	1.30	16
^6Li	II	222.3	1.21	0.800	11.8	2.017	1.035	1.30	16
α	III	46.6	1.40	0.55	15.7	1.40	0.50	1.25	17
α	IV	191.0	1.52	0.54	33.0	1.52	0.52	1.25	18

[a] $R = rA_T^{1/3}$.

TABLE III. Two-particle shell model configurations of states in ^{18}F.

E_x (MeV)	J^π	Allowed L values	Amplitudes [a] $(1d_{5/2})^2$	$(1d_{5/2},1d_{3/2})$	$(1d_{5/2},2s_{1/2})$	$(1d_{3/2})^2$	$(1d_{3/2},2s_{1/2})$	$(2s_{1/2})^2$
0.0	1^+	0,2	0.592	−0.667	···	−0.049	0.158	0.421
0.937	3^+	2,4	0.522	−0.243	0.818	0.021	···	···
1.122	5^+	4	1.00	···	···	···	···	···
3.725	1^+	0,2	−0.512	0.090	···	0.101	0.080	0.844
3.836	2^+	2	···	0.569	0.715	···	0.406	···

[a] T. T. S. Kuo and G. E. Brown, Nucl. Phys. 85, 140 (1966); C. Rolfs, W. E. Kieser, R. E. Azuma, and A. E. Litherland, Nucl. Phys. A199, 274 (1973).

calculations for all states are slightly out of phase with the data and do not predict the magnitude of the back angle cross section when normalizations were made to the forward angle data. The optical parameters in Sets II and IV for ^{6}Li and α were varied by 20% in calculations for the 1^+ state. The variation of the parameters did not result in better fits to the phase of the data or magnitude at back angles. All of the following results were obtained with optical potentials II and IV for ^{6}Li and α.

The nonlocal correction factor (PNLOC) with a value of 0.85 and a ^{6}Li rms radius of 2.18 found by White[1] to give the best fit to the ^{12}C(^{6}Li, α)^{14}N angular distributions are used here also. The bound state wave functions used in these calculations were generated from a Woods-Saxon potential as suggested by Philpott[22] from continuum shell model calculations for ^{16}O+$p(n)$. The geometrical parameters are listed in Table V. Variation of the geometrical potential parameters by as much as 50% did not result in any better fit to the phase of the experimental angular distributions, although the magnitude was affected by as much as 30% in some cases. The bound state parameters of Philpott were used in all further calculations.

The results of ZRTNT calculations normalized to the forward angle data for the population of the 1^+ (0.0 MeV), 3^+ (0.937 MeV), and (0^-,5^+) (1.1 MeV) levels of ^{18}F are shown in Figs. 8–10. The normalization factors range from 100–300 implying a value for D_0^2 of $(1-3)\times 10^6$ MeV fm^3. The fits to the data are not particularly good except at the extreme forward angles.

4. *Finite-range* DWBA *calculations*

The effects of including the finite extent of ^{6}Li were investigated in finite-range DWBA deuteron cluster transfer (FRDCT) calculations using the computer program MERCURY.[23] In the calculations the deuteron cluster was bound to the α-particle core in a Woods-Saxon potential with $r = 1.5$ fm and $a = 0.65$ fm as indicated in Table V. The use of a somewhat larger bound state radius for ^{6}Li, as suggested by Neudatchin and Smirnov,[24] is consistent with results obtained from electron scattering. The inclusion of the $1D$ component of ^{6}Li in these calculations did not contribute significantly to the differential cross section except where the cross section from the $2S$ component was at a minimum.

A comparison of FRDCT and ZRTNT calculations is shown in Fig. 8 for the 1^+ state. The FRDCT calculation does not predict the magnitude of the back angle cross section when normalized at forward angles. The ^{6}Li bound state geometry was

TABLE IV. Two-particle structure factors for ^{18}F [L. M. Polsky, C. H. Holbrow, and R. Middleton, Phys. Rev. 186, 966 (1969)].

E_x (MeV) Theory	E_x (MeV) Experimental	I_t^π	L_t	N_t [a] =	$G(N_tL_t, S=1, I_tT_t=0)$ 0	1	2
0.17	0.0	1^+	0		0.015	0.090	0.556
			2		0.008	0.097	···
0.96	0.937	3^+	2		0.058	0.592	···
			4		0.016	···	···
1.31	1.122	5^+	4		0.603	···	···
3.77	3.725	1^+	0		−0.005	0.081	−0.179
			2		−0.018	−0.119	···
3.41	3.836	2^+	2		0.056	0.563	···

[a] Node at the origin is not included.

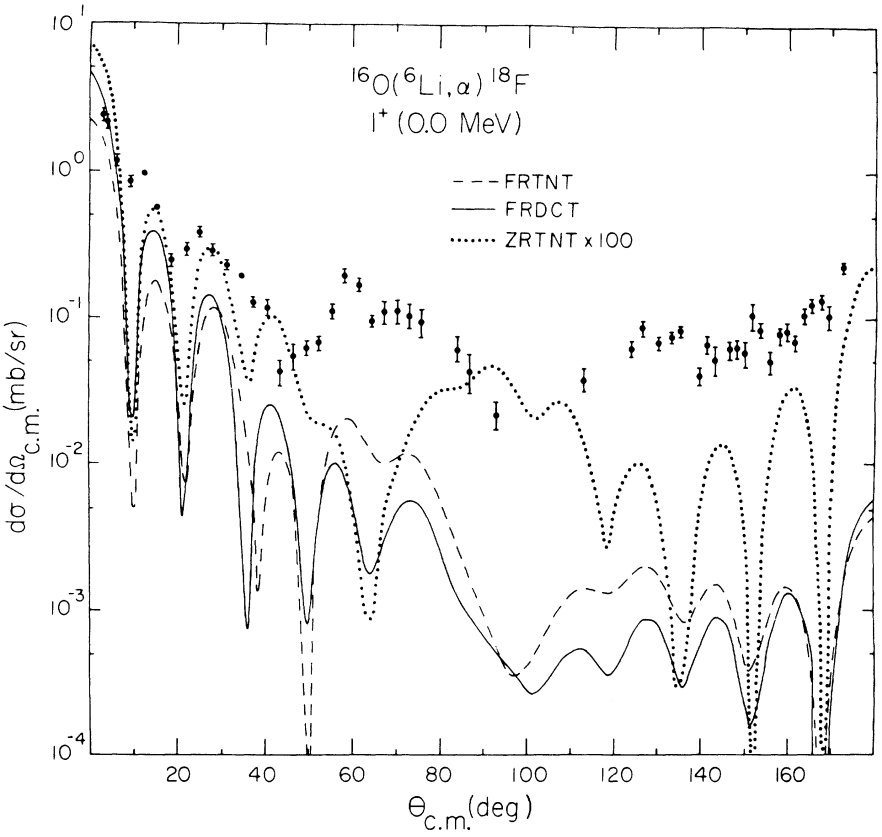

FIG. 8. Comparison between a zero-range DWBA two-particle transfer calculation (ZRTNT), a finite-range DWBA cluster form factor calculation (FRDCT), and a finite-range calculation using a two-particle form factor (FRTNT) for the 1^+ (0.0 MeV) state of ^{18}F.

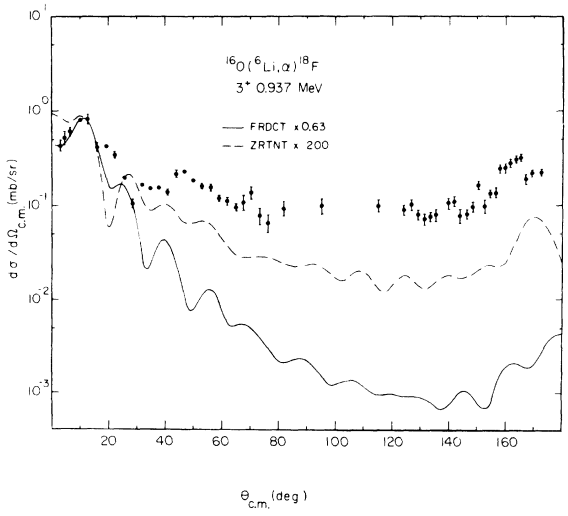

FIG. 9. Comparison of a zero-range two-particle DWBA calculation (ZRTNT) with a finite-range cluster form factor calculation (FRDCT) for the 3^+ (0.937 MeV) state of ^{18}F.

varied in a further attempt to fit the magnitude of the data at back angles. The phase does not change at forward angles when a larger (2.51 fm) radius is used, as shown in Fig. 11, while the various maxima change in magnitude with the larger radius. The back angle cross section is larger with the larger radius, but the absolute cross section at forward angles is lower and falls off faster.

A finite-range DWBA calculation (FRTNT), using two single-nucleon wave functions expanded in a harmonic oscillator series, was performed using the computer code TNT,[25] written by Charlton. The shell model wave functions of Kuo and Brown[3] were used for ^{18}F and a $(p)^2$ $L=0$, $S=1$, $T=0$ configuration for ^6Li was assumed. The ^6Li bound state parameters are those indicated by $\alpha+p(n)$ in Table V. The results of this calculation (FRTNT) are shown in Fig. 8 for the 1^+ state of ^{18}F. The magnitude and phase of the FRTNT and FRDCT calculations are similar at forward angles. There are, however, differences in magnitude at back angles. Compared with the data, both calculations are slightly out of phase and underpredict the forward

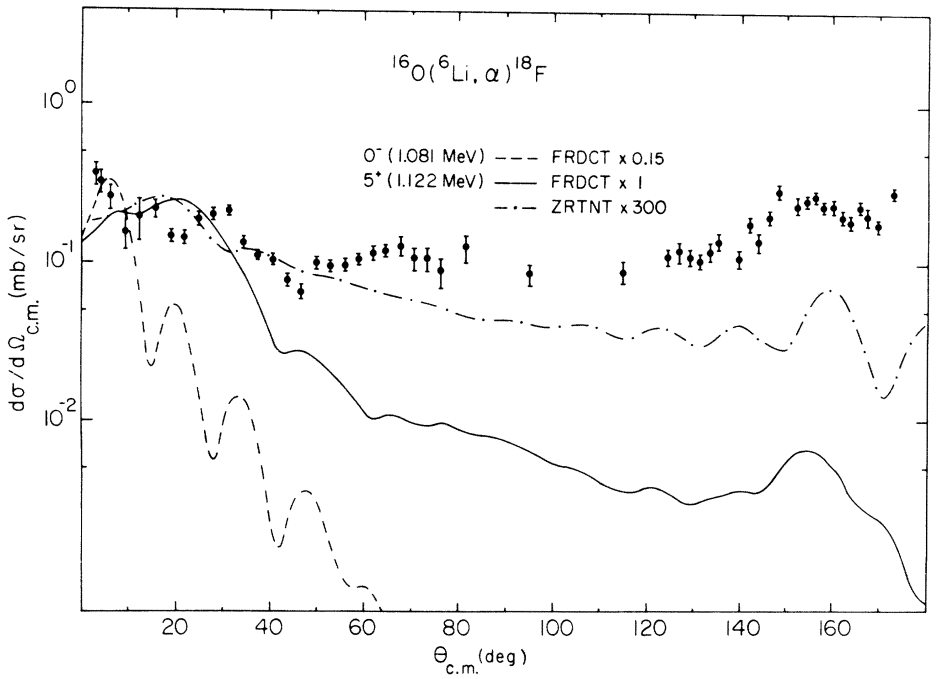

FIG. 10. Comparison of a zero-range DWBA calculation (ZRTNT) and a finite-range calculation (FRDCT) for the 0^- $+5^+$ (1.081 + 1.122 MeV) doublet in ^{18}F.

angle to backward angle ratio. Good fits to the data over the entire angular range *cannot* be attained with either FRTNT or FRDCT DWBA calculations.

FRDCT calculations were performed for the 3^+ (0.937 MeV), $5^+ + 0^-$ (1.1 MeV), 1^+ (3.725 MeV), and 2^+ (3.836 MeV) states, as shown in Figs. 9, 10, and 12. Normalization of the calculations to the data are indicated in the figures. The first maximum of the 3^+ angular distribution is fitted fairly well by both FRDCT and ZRTNT calculations, but the phase gradually becomes worse with increasing angle. The rise at forward angles in the $0^- + 5^+$ experimental angular distribution is due to the 0^- state. The first maximum of the 5^+ calculation as shown in Fig. 10 is 10° out of phase with the data. Angular distributions of forward angle data from the 1^+ (3.725 MeV) and 2^+ (3.836 MeV) states are shown in Fig. 12 with the FRDCT calculations. At these angles the 1^+, 2^+, and 3^- yields could be separated more completely because of better resolution. The cross section for the 3^- (3.791 MeV) state is indicated for two angles where yields could be obtained by fitting the peaks. A FRDCT calculation for the 2^- (2.101 MeV) level, assuming a $2F$ and $3P$ cluster configuration, is shown in Fig. 13. As can be seen, the L transfer for this state can only be distinguished at angles forward of 5° lab where it was impossible to obtain data because of the high background, small cross section.

5. *Absolute magnitudes*

The real test of shell model wave functions in reaction studies is that of predicting the absolute magnitude of the differential cross section with DWBA calculations. The factors necessary to normalize the FRDCT, FRTNT, and ZRTNT calcula-

TABLE V. Bound state parameters (the potential well depths were varied until the proper binding energies were attained).

Particle + core	E_B [a] (MeV)	r (fm)	a (fm)	γ_{so}	r_c (fm)	PNLOC	^{6}Li rms radius (fm)
$p(n) + {}^{16}O$	$+3.76 - E_x$ [a]	1.00	0.65	•••	1.25	0.85	2.18
$d + {}^{16}O$	$+7.53 - E_x$ [a]	1.40	0.65	25	1.25	•••	•••
$p(n) + \alpha$	0.74	1.50	0.65	25	1.25	•••	•••
$d + \alpha$	1.47	1.51	0.65	25	1.30	•••	•••

[a] The proton and neutron binding energies were assumed to be identical and equal to half the deuteron binding energy. The excitation energies E_x were subtracted to give the binding energy for the excited states.

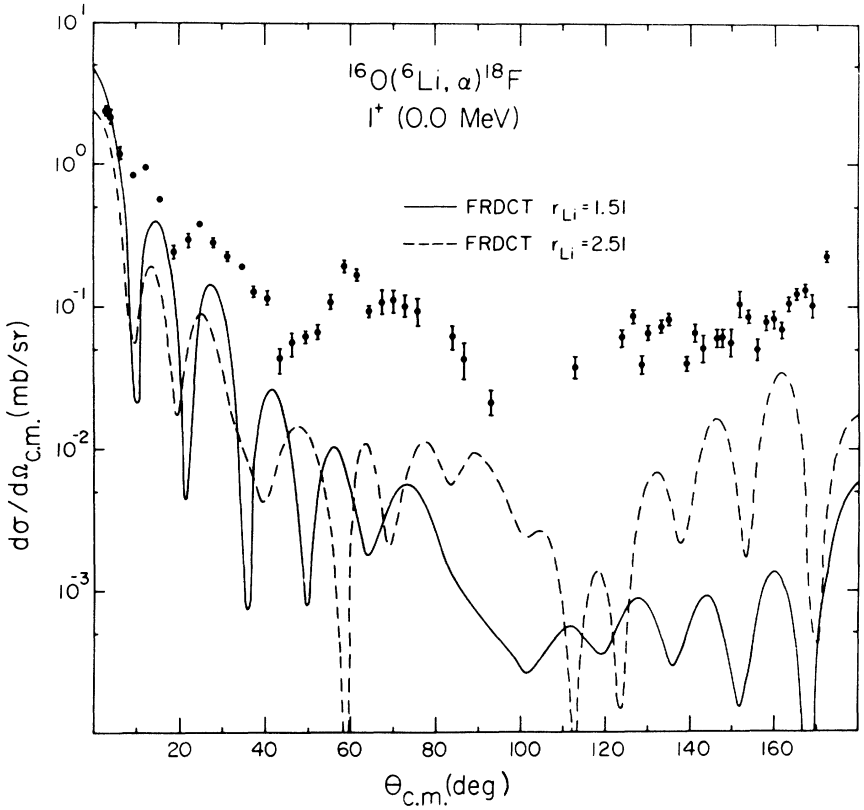

FIG. 11. Comparison of FRDCT calculations for the 1^+ (0.0 MeV) state of ^{18}F using two different ^6Li bound state radii (r_{Li}), where $R = r_{Li} A_T^{1/3}$.

tions to the first maximum of the data are given in Table VI. The magnitude of the first 1^+, 3^+, and 5^+ states, whose structure is well known, is predicted to within a factor of 2 for FRDCT calculations. For the 5^+ angular distribution, the normalization factor is 1 at the second maximum. It is quite important for the 1^+ and 3^+ states to have data forward of 20° in order to obtain the true normalization. This is most apparent for the 3^+ (0.937 MeV) state as shown in Fig. 9. The magnitude of the first maximum is fitted well with a normalization of 0.63, while the second maximum of the FRDCT calculation is entirely out of phase with the data.

The ZRTNT calculations predict the absolute cross section with a consistent normalization factor of 100 to 300 for all states. Since the ratios of magnitudes of zero-range and finite-range calculations are essentially constant, the much faster ZRTNT calculation with a normalization factor of 100 might provide reasonable estimates of absolute cross sections for other $(^6Li, \alpha)$ reactions. However, other $(^6Li, \alpha)$ studies are needed to check this.

6. *Reaction mechanisms*

The difficulties encountered in fitting the angular distributions of the 1^+, 3^+, and 5^+ states were also encountered by White *et al.*[2] in a DWBA analysis of the $^{12}C(^6Li, \alpha)^{14}N$ reaction. In the $^{12}C(^6Li, \alpha)^{14}N$ reaction the difficulties were attributed to contributions occurring from stripping to ^{14}N from the 2^+ first excited state in ^{12}C. The inclusion of inelastic scattering in the $(^6Li, \alpha)$ angular distributions to 1^+ states from the 3^- state in ^{16}O would produce different contributions than would be produced by the inclusion of the 2^+ state in the ^{12}C case. However, the shape of the 1^+ state angular distributions to ^{14}N and ^{18}F with similar nuclear structure were observed to be similar. It would seem then that the inability to describe the $^{16}O(^6Li, \alpha)^{18}F$ and $^{12}C(^6Li, \alpha)^{14}N$ reactions cannot be attributed solely to multistep contributions. In addition to this it was already concluded that compound nuclear processes cannot explain the problem.

The back angle peaking of light ion reactions on $1p$ shell nuclei has been explained by Werby

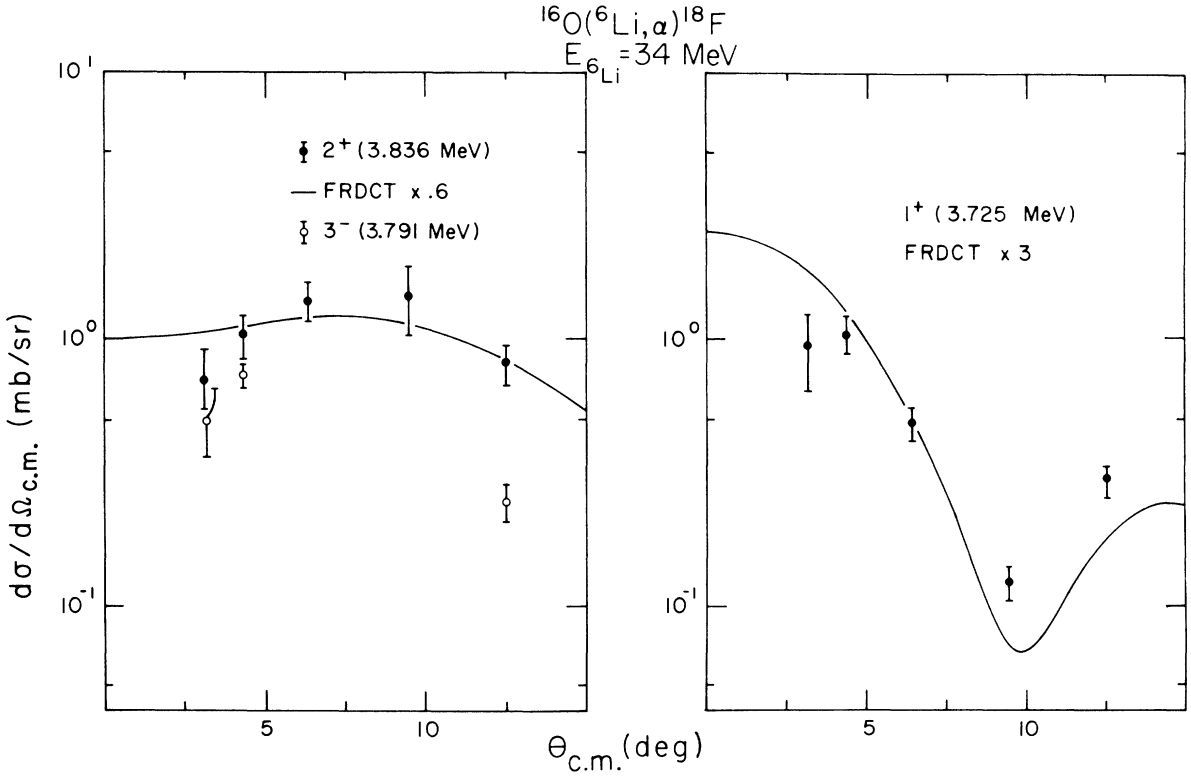

FIG. 12. Forward angle angular distributions for the 1^+ (3.725 MeV) and 2^+ (3.836 MeV) states in ^{18}F and FRDCT calculations. The differential cross section for the 3^- (3.791 MeV) state is shown at the two angles where it could be reliably extracted.

et al.[15,26,27] and by Bohlen, Marquardt, and Von Oertzen[28] in terms of exchange effects. Because of the strong clustering in ^{16}O, the $(^6Li,\alpha)$ reaction may have large exchange contributions. In order to see what the shape of the exchange angular distribution might be, the $^6Li(^{16}O,\alpha)^{18}F$ reaction calculation was performed with MERCURY. This calculation does not include the direct amplitude, and the interaction potential was simplified to include only the $^{12}C+\alpha$ potential. The wave function for $^{16}O(^{12}C+\alpha)$ was assumed to be $4S$, while that of $^{18}F(^{12}C+^6Li)$ was assumed to have $5S$ and $4D$ components. The resulting cross section was backward peaked and flat elsewhere. This same observation has been made by Werby and Tobocman,[29] who are investigating the exchange terms in detail. It is hoped that inclusion of exchange amplitudes will enable a more complete understanding of the $(^6Li,\alpha)$ reaction.

V. CONCLUSIONS

The positive parity states in ^{18}F, which can be described as a closed ^{16}O core plus two nucleons in the $(2s,1d)$ shell, are the most strongly populated states in the $^{16}O(^6Li,\alpha)^{18}F$ reaction. Compound nuclear contributions have been shown to be small. The general structure of the forward angle data can be reproduced by zero-range DWBA calculations, although the calculations are out of phase with the data. The magnitude of the data at back angles is at least an order of magnitude greater than predicted by the DWBA calculations. The finite-range fits to the data were not significantly better than the zero-range fits and the effect of the $1D$ state in ^6Li was minimal. In fact, the $1D$ amplitude would have to be at least 3 times larger to significantly affect the cross section.

The shape of the 1^+ (0.0 MeV), 3^+ (0.937 MeV), 1^+ (3.725 MeV), and 2^+ (3.836 MeV) states were in fair agreement with the calculations for angles less than 20° (c.m.) so that L-transfer determination can be made with forward angle data. Finite-range DWBA calculations using either cluster form factors or two-particle form factors produce equivalent fits to the magnitude and shape of the data. The zero-range DWBA calculations can also be used to calculate absolute cross sections, since the zero-range normalization constant is consistently between 100 and 200. From the 5^+ state, whose structure is best known in ^{18}F, the value of the zero-range normalization constant is 100. The

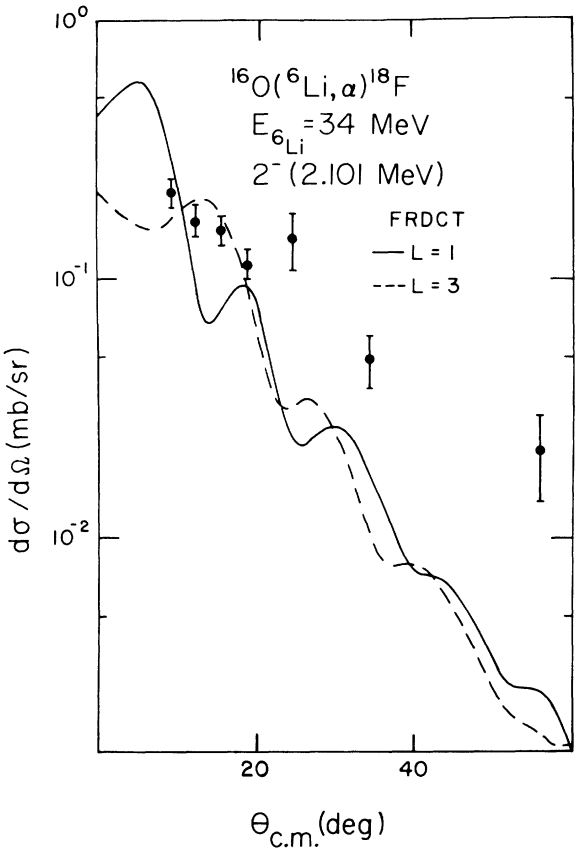

FIG. 13. Angular distribution for the 2^- (2.101 MeV) state of ^{18}F with FRDCT calculations.

TABLE VI. DWBA normalization factors.

E_x	J^π	ZRTNT	FRDCT	FRTNT
0.0	1^+	100–300	1.0–2.0	1.0–2.0
0.937	3^+	200	0.6–1.0	•••
1.122	5^+	100–300	0.8–1.0	•••
3.725	1^+	100–300	1.0–3.0	•••
3.836	2^+	60–100	0.6–1.0	

wave functions of Kuo and Brown,[3] when used in DWBA calculations, predict the magnitudes for the 1^+ (0.0 MeV), 3^+ (0.937 MeV), and 2^+ (3.836 MeV) states in ^{18}F to within a factor of 2.

Similar difficulties to those found in the present work occurred for the $^{12}C(^6Li,\alpha)^{14}N$ reaction[1,2] where the phase problems were attributed to the contribution of inelastic excitation of the target to the transfer cross sections. However, since these difficulties are encountered in the $(^6Li,\alpha)$ reaction on ^{16}O, it would seem that multistep contributions from inelastic excitation are not the primary source of difficulty in the $(^6Li,\alpha)$ reaction. The anomalies in the DWBA fits to the experimental angular distributions may possibly be explained by the inclusion of the exchange of an α particle in ^{16}O with the ^6Li projectile.

The authors wish to thank L. A. Charlton, F. Petrovich, and D. Robson for extremely instructive discussions, and G. M. Hudson, R. J. Puigh, M. E. Williams-Norton, and A. F. Zeller for their aid in taking the data.

†Work supported in part by National Science Foundation Grants Nos. NSF-PHY-7503767-A01, NSF-GU-2612, and NSF-GJ-367.

*Present address: Physics Department, University of Pennsylvania, Philadelphia, Pennsylvania 19174.

[1]R. L. White, K. W. Kemper, L. A. Charlton, and W. J. Courtney, Phys. Rev. Lett. 31, 254 (1973).
[2]R. L. White, L. A. Charlton, and K. W. Kemper, Phys. Rev. C 12, 1918 (1975).
[3]T. T. S. Kuo and G. E. Brown, Nucl. Phys. 85, 40 (1966).
[4]L. M. Polsky, C. H. Holbrow, and R. Middleton, Phys. Rev. 186, 966 (1969).
[5]N. F. Mangelson, B. G. Harvey, and N. K. Glendenning, Nucl. Phys. A119, 79 (1968).
[6]K. R. Chapman, Nucl. Instrum. Methods 124, 299 (1975).
[7]G. R. Morgan, G. D. Gunn, M. B. Greenfield, N. R. Fletcher, J. D. Fox, D. L. McShan, and Lon Wright, Nucl. Instrum. Methods 123, 439 (1975).
[8]G. D. Gunn, T. A. Schmick, L. Wright, and J. D. Fox, Nucl. Instrum. Methods 113, 1 (1973).
[9]S. R. Salisbury, G. Hardie, L. Opplinger, and R. Dangle, Phys. Rev. 126, 2143 (1962).
[10]F. Ajzenberg-Selove, Nucl. Phys. A140, 1 (1972).
[11]F. Pühlhofer and R. Bock, Phys. Lett. 25B, 117 (1967).
[12]N. F. Mangelson, B. G. Harvey, and N. K. Glendenning, Nucl. Phys. A117, 161 (1968).
[13]G. E. Moore, M.S. thesis, Florida State University, 1972 (unpublished).
[14]G. R. Satchler, Nucl. Phys. 55, 1 (1964).
[15]M. F. Werby, M. B. Greenfield, K. W. Kemper, D. L. McShan, and S. Edwards, Phys. Rev. C 8, 106 (1973).
[16]P. Schumacher, N. Ueta, H. H. Duhm, K. I. Kubo, and W. J. Klages, Nucl. Phys. A212, 573 (1973).
[17]B. G. Harvey, J. R. Meriwether, and J. Mahoney, Phys. Rev. 146, 712 (1966).
[18]L. F. Hansen, H. F. Lutz, M. L. Stelts, J. G. Vidal, and J. J. Wesolowski, Phys. Rev. 158, 917 (1967).
[19]A. W. Obst and K. W. Kemper, Phys. Rev. C 9, 1643 (1974).
[20]P. D. Kunz, Fortran IV program DWUCK, University of Colorado, Boulder, Colorado, 1969 (unpublished).
[21]B. F. Bayman and A. Kallio, Phys. Rev. 156, 1121 (1967).
[22]R. J. Philpott, Phys. Rev. C 5, 1457 (1972).

[23]L. A. Charlton and D. Robson, Florida State University Technical Report No. 5 (unpublished).
[24]V. G. Neudatchin and Yu. F. Smirnov, *Progress in Nuclear Physics* (Pergamon, New York, 1969), Vol. 10, p. 273.
[25]L. A. Charlton, Nucl. Phys. A241, 144 (1975).
[26]M. F. Werby and S. Edwards, Phys. Rev. C 8, 978 (1973); M. B. Greenfield, M. F. Werby, and R. J. Philpott, *ibid.* 10, 564 (1974).
[27]S. Edwards, D. Robson, T. L. Talley, W. J. Thompson, and M. F. Werby, Phys. Rev. C 8, 456 (1973); M. Werby and S. Edwards, Nucl. Phys. A213, 294 (1973).
[28]H. Bolen, N. Marquardt, and W. von Oertzen, Nucl. Phys. A179, 504 (1972).
[29]M. F. Werby and W. Tobocman, Bull. Am. Phys. Soc. 20, 688 (1975).